Laplace transform integration of the shallow water equations. Part 1: Eulerian formulation and Kelvin waves

Colm Clancy* and Peter Lynch
School of Mathematical Sciences, UCD, Belfield, Dublin 4, Ireland
*Correspondence to: School of Mathematical Sciences, UCD, Belfield, Dublin 4, Ireland. E-mail: Colm.Clancy@ucd.ie

A filtering integration scheme is developed, using a modification of the contour used to invert the Laplace transform (LT). It is shown to eliminate components with frequencies higher than a specified cut-off value. Thus it is valuable for integrations of the equations governing atmospheric flow. The scheme is implemented in a shallow water model with an Eulerian treatment of advection. It is compared to a reference model using the semi-implicit (SI) scheme. The LT scheme is shown to treat dynamically important Kelvin waves more accurately than the SI scheme. Copyright © 0000 Royal Meteorological Society

Key Words: Numerical weather prediction; Time integration; Filtering

Received . . .

Citation: . . .

1. Introduction

The purpose of this work is to investigate a filtering integration technique suitable for application to a range of physical problems, in particular to numerical weather prediction. In operational NWP, efficiency is crucial, as we must produce regular and timely forecasts. In integrating the equations of motion, we need to use the longest timestep possible while still retaining acceptable accuracy.

Explicit finite difference schemes are limited by the CFL criterion, as stability is governed by the fastest waves present in the system. Fully implicit methods lead to complicated coupled nonlinear systems, which are impractical to solve in an operational context. The development of the semi-implicit method by Robert (1969) was a major breakthrough. By averaging terms leading to fast-moving gravity waves, Robert was able to achieve acceptable accuracy using a time step considerably larger than that required for explicit methods.

Despite these advances, there remain a number of issues with the semi-implicit method. In particular, the method maintains stability by slowing down the fast-moving waves in the system (see, e.g., Lynch, 2006, pp. 85–87). This may be problematic if we need to simulate a phenomenon that is influenced by such waves. Every discretisation technique invariably has its own strengths and weaknesses and there is still no 'perfect' scheme. It is important, therefore, that research into numerical methods for atmospheric models is continued. With this motivation we investigate a numerical scheme that offers some significant advantages over existing schemes.

High frequency noise has been a problem throughout the history of NWP. As outlined in Lynch (2006), this was the main cause of the failure of Richardson's forecast. Various initialization techniques have been developed to address this problem. One such method, first presented in Lynch (1985a, 1985b), used a modified inversion to the Laplace transform (LT) to remove high frequency components from the initial conditions. The LT initialization scheme was reviewed in Daley (1991). In Van Isacker and Struylaert (1985), Lynch (1986) and Lynch (1991), this method was extended beyond initialization and a filtering time-stepping scheme was developed from the idea. The work presented in this paper further develops the LT discretisation as a viable numerical scheme for NWP. The implementation of the scheme is described and the benefits of the technique over existing schemes are demonstrated by a combination of analytical and numerical approaches.

This study is presented in two parts. In Part 1 we implement an LT scheme in a model using Eulerian advection and demonstrate its advantages for simulating atmospheric waves, in particular Kelvin waves. In Part 2 (Clancy and Lynch, 2011) we combine the LT scheme with a semi-Lagrangian advection scheme. We show that it is accurate and that it is free from the problem of orographic resonance that is found with semi-implicit schemes.

In §2, the background theory and mathematical formulation of the LT integration scheme is presented. After these preliminaries, we test the LT method's efficacy as a numerical solver for the partial differential equations governing the atmosphere. In §3, a spectral model using the LT method for its temporal discretisation is developed, using an existing shallow water model (STSWM) as a basis and reference. The scheme is evaluated using various standard test cases. Along with a linear analysis in a simple oscillation equation, we perform shallow water simulations of Kelvin waves to investigate the effect of the LT scheme on phase speeds and, in §4, demonstrate its benefits over the semi-implicit scheme. Finally, a summary of the main results and conclusions is given in §5.

2. The Laplace transform integration method

2.1. Basic definitions

Given a function $f(t)$ with $t \geq 0$, the Laplace transform (LT) is defined as

$$\widehat{f}(s) \equiv \mathfrak{L}\{f\} = \int_0^\infty e^{-st} f(t)\,\mathrm{d}t \tag{1}$$

The variable s is complex. The inversion from a transformed function back to the original is given by the contour integral

$$f(t) \equiv \mathfrak{L}^{-1}\{\widehat{f}\} = \frac{1}{2\pi i}\int_{\mathcal{C}} e^{st}\widehat{f}(s)\,\mathrm{d}s \tag{2}$$

where the contour $\mathcal{C}$ is a line parallel to the imaginary axis in the s-plane, to the right of all the singularities of $\widehat{f}$. Further theory and applications of the Laplace transform may be found in Doetsch (1971).

The ability of the Laplace transform to filter high frequencies is illustrated by the simple example of a function consisting of a slow and a fast oscillation. We define

$$f(t) = a\,e^{i\,\nu_R\,t} + A\,e^{i\,\nu_G\,t}$$

with $|\nu_R| \ll |\nu_G|$. The LT of this function is given by

$$\widehat{f}(s) = \frac{a}{s - i\,\nu_R} + \frac{A}{s - i\,\nu_G}.$$

The function $\widehat{f}$ has two simple poles on the imaginary axis, at $s = i\,\nu_R$ and $s = i\,\nu_G$. To invert this to $f(t)$ we would normally use the inversion integral (2) along the straight line $\mathcal{C}$ shown in Figure 1 (left panel).

To remove the high frequency component, we choose a positive real number γ such that $|\nu_R| < \gamma < |\nu_G|$. Then we define a closed contour $\mathcal{C}^*$ as the circle centred at the origin, with radius γ, as depicted on the left in Figure 1. We replace $\mathcal{C}$ by $\mathcal{C}^*$ in the integral in (2), yielding the modified inversion

$$f^*(t) \equiv \mathfrak{L}^*\{\widehat{f}\} = \frac{1}{2\pi i}\oint_{\mathcal{C}^*} e^{st}\widehat{f}(s)ds \tag{3}$$

The function $f^*(t)$ contains only contributions from the poles lying within $\mathcal{C}^*$, that is, those with frequencies less than γ. From Cauchy's Integral Formula we readily find that

$$f^*(t) = a\,e^{i\,\nu_R\,t}$$

Thus, the modified inversion integral (3) acts to filter high frequency behaviour, as required.

2.2. Laplace transform integration

The LT method was originally used as an initialisation technique (Lynch, 1985a,b). The extension to time integration was studied in Van Isacker and Struylaert (1985, 1986) and Lynch (1986, 1991). The basic idea is to consider the LT over a discrete interval of time Δt. The transforms can be computed analytically and the modified inversion operator (3) is applied to find a filtered value at the end of the interval. We consider the transform of the general equation

$$\frac{\mathrm{d}\mathbf{X}}{\mathrm{d}t} + \mathbf{L}\mathbf{X} + \mathbf{N}(\mathbf{X}) = 0$$

where $\mathbf{L}$ is a linear operator and $\mathbf{N}$ a nonlinear vector function, and rearrange to get

$$\widehat{\mathbf{X}} = (s\mathbf{I} + \mathbf{L})^{-1}[\mathbf{X}^0 - \mathbf{N}^0/s] \tag{4}$$

The initial value is $\mathbf{X}^0$ and we have held the nonlinear term at its initial value $\mathbf{N}^0$. We apply the inversion operator at time $t = \Delta t$ to get the filtered state at this time

$$\mathbf{X}(\Delta t) = \mathfrak{L}^*\left\{\widehat{\mathbf{X}}\right\}\Big|_{t=\Delta t}$$

Having the solution at $t = \Delta t$ we continue stepwise to extend the forecast. In general we consider the time interval $[\tau\Delta t, (\tau+1)\Delta t]$. The filtered solution at time $(\tau+1)\Delta t$ is found by applying the modified inversion to the LT of the equation. Over this general interval, the 'initial condition' in (4) will be taken at the beginning of the interval, that is, $\mathbf{X}^\tau \equiv \mathbf{X}(\tau\Delta t)$. The nonlinear terms are also evaluated at this time. Thus the solution at time $(\tau+1)\Delta t$ is

$$\mathbf{X}^{\tau+1} = \mathfrak{L}^*\{(s\mathbf{I} + \mathbf{L})^{-1}[\mathbf{X}^\tau - \mathbf{N}^\tau/s]\}\Big|_{t=\Delta t}$$

Alternatively, a centred approach may be taken, where we consider the interval $[(\tau-1)\Delta t, (\tau+1)\Delta t]$ and the nonlinear terms are evaluated at the centre $\tau\Delta t$. The general forecasting procedure is thus as follows:

$$\begin{aligned}\widehat{\mathbf{X}}(s) &= (s\mathbf{I} + \mathbf{L})^{-1}\left[\mathbf{X}^{\tau-1} - \mathbf{N}^\tau/s\right]\\ \mathbf{X}^{\tau+1} &= \mathfrak{L}^*\left\{\widehat{\mathbf{X}}\right\}\Big|_{t=2\Delta t}\end{aligned} \tag{5}$$

Care must be taken to ensure that $(s\mathbf{I} + \mathbf{L})^{-1}$ exists. The matrix $s\mathbf{I} + \mathbf{L}$ is singular when we have $s = -\lambda$, for λ an eigenvalue of $\mathbf{L}$. But $|s| = \gamma$, the radius of the contour $\mathcal{C}^*$. The problem can thus be avoided by a suitable choice of γ, the cutoff frequency.

2.3. Evaluating the contour integral

The inversion using $\mathfrak{L}^*$ requires the complex integration in (3), around the circle $\mathcal{C}^*$. To apply the filter in practice, we replace $\mathcal{C}^*$ by the N-sided polygon $\mathcal{C}^*_N$ to reduce the integration to a summation. The length of each edge is Δs_n and the midpoints are labelled s_n for $n = 1, 2, \ldots, N$. The right panel of Figure 1 shows the case with $N = 8$.

We can now define the numerical operator used for the modified inversion as

$$\mathfrak{L}^*_N\{\widehat{f}\} \equiv \frac{1}{2\pi i}\sum_{n=1}^{N} e^{s_n t}\widehat{f}(s_n)\Delta s_n$$

It was suggested in Van Isacker and Struylaert (1985) that the exponential term in the expression for the numerical inversion should be replaced by a Taylor series truncated to N terms. We write

$$e_N^z = \sum_{j=0}^{N-1} \frac{z^j}{j!} \tag{6}$$

If we divide the summation in the numerical inversion by

$$\kappa = \frac{N}{\pi} \tan \frac{\pi}{N}$$

then the inversion is exact for a constant function, and for any power of t up to degree $N-1$ (Clancy, 2010).

As noted in Lynch (1991), it can be shown that

$$1/\kappa = (2\pi i/N)\,(s_n/\Delta s_n)$$

so the final form of the numerical filtering inversion integral to be used is

$$\mathfrak{L}_N^*\{\,\widehat{f}\,\} \equiv \frac{1}{N} \sum_{n=1}^{N} e_N^{s_n t}\, \widehat{f}(s_n)\, s_n \tag{7}$$

2.4. *Filter response and stability*

With the inversion operator $\mathfrak{L}_N^*$ defined by (7), we consider the effect of the filtering operator $\mathfrak{L}_N^*\mathfrak{L}$ on a single wave component $f(t) = e^{i\omega t}$. This was analysed by Van Isacker and Struylaert (1985) and Lynch (1986), who showed that

$$\mathfrak{L}_N^*\mathfrak{L}\left\{e^{i\omega t}\right\} = H_N(\omega)\, e_N^{i\,\omega\,t} \tag{8}$$

where

$$H_N(\omega) = \frac{1}{1 + \left(\dfrac{i\,\omega}{\gamma}\right)^N} \tag{9}$$

If we always choose a value for N that is a multiple of 4, we ensure that $H_N(\omega)$ is real and $|H_N(\omega)| \le 1$. Thus its effect is to damp the input, without a phase shift. In addition, the operator $\mathfrak{L}_N^*\mathfrak{L}$ truncates the original $e^{i\,\omega\,t}$ to N terms. We note the H_N is the square of the response function of a Butterworth lowpass filter (Oppenheim and Schafer, 1989).

Lynch (1986) showed how, when the centred LT method given by (5) is used, the response above yields the sufficient stability criterion

$$\Delta t \le \frac{(N!)^{1/N}}{2\gamma} \tag{10}$$

This is a very lenient condition. With typical value $N = 8$ and a cut-off frequency defined by a period $\tau_c = 6$ hours, we get a maximum timestep of around 1.8 hours, longer than would normally be used in practice.

3. The spectral transform shallow water model

We now test the performance of the LT integration scheme in a shallow water model. A key benefit of the LT method is stability, with its potential to allow long timesteps to be used. We will compare it with a reference semi-implicit method.

When the shallow water equations are discretised with a semi-implicit scheme, one obtains a Helmholtz equation that needs to be solved at every timestep. Clearly an efficient solver is essential. When the LT method is applied, we encounter an analogous Helmholtz equation. Whereas the semi-implicit method requires the solution of the equation once every timestep, for the LT scheme we must solve it at each of the N midpoints on an N-gon. It is vital that the benefits of the LT scheme are not negated by the extra computational overhead. This motivates the coupling of the LT scheme with the spectral transform method, for which the solution of a Helmholtz equation is simple and efficient.

The spectral transform method uses spherical harmonics as basis functions for expansion of the model fields. Spherical harmonics are the eigenfunctions of Laplace's equation and satisfy

$$\nabla^2 Y_\ell^m = -\frac{\ell(\ell+1)}{a^2} Y_\ell^m \tag{11}$$

where a is the radius of the Earth. Writing $\mu = \sin\phi$, they are defined by $Y_\ell^m(\lambda,\mu) = e^{im\lambda}\, P_\ell^m(\mu)$. The P_ℓ^m are the associated Legendre functions. Washington and Parkinson (2005) provide the further details of spherical harmonics that are necessary for the spectral transform method.

Examining (11) we see that computing the Laplacian of a series of spherical harmonics merely requires scalar multiplications. The solution of a Helmholtz equation is therefore computationally trivial. This provides the motivation for using the spectral transform method with a LT time integration.

3.1. *STSWM: Basic equations*

The Spectral Transform Shallow Water Model (STSWM) is a freely available model developed at the National Center for Atmospheric Research (NCAR) and described in Hack and Jakob (1992). It is designed to solve the shallow water equations using a spectral transform method and specifically to consider the test suite of Williamson et al. (1992). The original code is written in Fortran 77. An updated version in Fortran 90 was developed by the ICON group at the Max Planck Institute for Meteorology (MPI-M) and the Deutscher Wetterdienst (DWD) [`http://icon.enes.org/`].

We now provide a brief overview of the model's discretisation. Full details are given in the report of Hack and Jakob. Jakob et al. (1993) specifically describe the changes needed to include orography in the model.

The shallow water equations are given in the form

$$\begin{aligned}
\frac{\partial \eta}{\partial t} &= -\frac{1}{a(1-\mu^2)}\frac{\partial}{\partial\lambda}(U\eta) - \frac{1}{a}\frac{\partial}{\partial\mu}(V\eta) \\
\frac{\partial \delta}{\partial t} &= \frac{1}{a(1-\mu^2)}\frac{\partial}{\partial\lambda}(V\eta) - \frac{1}{a}\frac{\partial}{\partial\mu}(U\eta) \\
&\quad - \nabla^2\left(\Phi_s + \Phi' + \frac{U^2+V^2}{2(1-\mu^2)}\right) \\
\frac{\partial \Phi'}{\partial t} &= -\frac{1}{a(1-\mu^2)}\frac{\partial}{\partial\lambda}(U\Phi') - \frac{1}{a}\frac{\partial}{\partial\mu}(V\Phi') - \bar{\Phi}^*\delta
\end{aligned} \tag{12}$$

Here $(U,V) = (u\cos\phi, v\cos\phi)$ are the horizontal wind images, $\mu = \sin\phi$, $\eta = \zeta + f$ is the absolute vorticity and δ is the horizontal divergence. The free surface geopotential

has been written as $\Phi = \bar{\Phi}^* + \Phi' + \Phi_s$, where $\bar{\Phi}^*$ is a time-independent spatial mean geopotential depth and Φ_s is the geopotential of the surface of the Earth.

All of the fields are represented as truncated series of spherical harmonics; for example, with a triangular truncation,

$$\eta(\lambda, \mu, t) = \sum_{\ell=0}^{L} \sum_{m=-\ell}^{\ell} \eta_\ell^m(t)\, e^{im\lambda}\, P_\ell^m(\mu)$$

Here η_ℓ^m are the time-dependent spectral coefficients. For the spectral transform method, the nonlinear terms on the right-hand side of (12) are computed in physical space and the product is then expanded in a series. Orthogonality of the spherical harmonics can then be used to obtain a series of equations for the spectral coefficients. We are left with a set of ordinary differential equations of the form

$$\begin{aligned} \frac{\mathrm{d}}{\mathrm{d}t}\eta_\ell^m &= \mathcal{N}_\ell^m \\ \frac{\mathrm{d}}{\mathrm{d}t}\delta_\ell^m &= \mathcal{D}_\ell^m + \frac{\ell(\ell+1)}{a^2}\,\Phi_\ell^m \\ \frac{\mathrm{d}}{\mathrm{d}t}\Phi_\ell^m &= \mathcal{F}_\ell^m - \bar{\Phi}^*\,\delta_\ell^m \end{aligned} \tag{13}$$

Note that the Φ_ℓ^m are the spectral coefficients of the perturbation geopotential Φ'; the prime has been dropped for ease of notation.

3.2. STSWM: Semi-implicit scheme

We use the semi-implicit STSWM as the reference model in this work. The discretisation of (13) is given by

$$\begin{aligned} \frac{\{\eta_\ell^m\}^{\tau+1} - \{\eta_\ell^m\}^{\tau-1}}{2\,\Delta t} &= \{\mathcal{N}_\ell^m\}^\tau \\ \frac{\{\delta_\ell^m\}^{\tau+1} - \{\delta_\ell^m\}^{\tau-1}}{2\,\Delta t} &= \{\mathcal{D}_\ell^m\}^\tau \\ &\quad + \frac{\ell(\ell+1)}{a^2}\,\frac{\{\Phi_\ell^m\}^{\tau+1} + \{\Phi_\ell^m\}^{\tau-1}}{2} \\ \frac{\{\Phi_\ell^m\}^{\tau+1} - \{\Phi_\ell^m\}^{\tau-1}}{2\,\Delta t} &= \{\mathcal{F}_\ell^m\}^\tau \\ &\quad - \bar{\Phi}^*\,\frac{\{\delta_\ell^m\}^{\tau+1} + \{\delta_\ell^m\}^{\tau-1}}{2} \end{aligned}$$

Here the superscript τ represents the discrete time level $t = \tau\,\Delta t$. The decoupling of the expressions for $\{\delta_\ell^m\}^{\tau+1}$ and $\{\Phi_\ell^m\}^{\tau+1}$ is simplified due to the spectral form of the Laplacian operator. The final time-stepping procedure can then be written as

$$\begin{aligned} \{\eta_\ell^m\}^{\tau+1} &= \{\eta_\ell^m\}^{\tau-1} + 2\,\Delta t\,\{\mathcal{N}_\ell^m\}^\tau \\ \{\delta_\ell^m\}^{\tau+1} &= \frac{1}{d}\left(\mathcal{R} + \mathcal{Q}\,\frac{\ell(\ell+1)}{a^2}\,\Delta t\right) \\ \{\Phi_\ell^m\}^{\tau+1} &= \frac{1}{d}\left(\mathcal{Q} - \mathcal{R}\,\bar{\Phi}^*\,\Delta t\right) \end{aligned} \tag{14}$$

where

$$\begin{aligned} d &= 1 + \bar{\Phi}^*\,\frac{\ell(\ell+1)}{a^2}\,\Delta t^2 \\ \mathcal{R} &= \{\delta_\ell^m\}^{\tau-1} + 2\,\Delta t\{\mathcal{D}_\ell^m\}^\tau + \Delta t\,\frac{\ell(\ell+1)}{a^2}\,\{\Phi_\ell^m\}^{\tau-1} \\ \mathcal{Q} &= \{\Phi_\ell^m\}^{\tau-1} + 2\,\Delta t\{\mathcal{F}_\ell^m\}^\tau - \Delta t\,\bar{\Phi}^*\,\{\delta_\ell^m\}^{\tau-1} \end{aligned}$$

3.3. STSWM: Laplace transform formulation

We now adapt the STSWM code to solve the shallow water equations using the LT method. Again we consider the system of equations (13) for the time-dependent spectral coefficients. We take the Laplace transform of each equation, as described in §2.2:

$$\begin{aligned} s\,\widehat{\eta_\ell^m} - \{\eta_\ell^m\}^{\tau-1} &= \frac{1}{s}\,\{\mathcal{N}_\ell^m\}^\tau \\ s\,\widehat{\delta_\ell^m} - \{\delta_\ell^m\}^{\tau-1} &= \frac{1}{s}\,\{\mathcal{D}_\ell^m\}^\tau + \frac{\ell(\ell+1)}{a^2}\,\widehat{\Phi_\ell^m} \\ s\,\widehat{\Phi_\ell^m} - \{\Phi_\ell^m\}^{\tau-1} &= \frac{1}{s}\,\{\mathcal{F}_\ell^m\}^\tau - \bar{\Phi}^*\,\widehat{\delta_\ell^m} \end{aligned}$$

As outlined previously, we are taking our 'initial' value at the beginning of the time step, i.e. at $t = (\tau-1)\,\Delta t$. The nonlinear terms $\mathcal{N}_\ell^m$, $\mathcal{D}_\ell^m$ and $\mathcal{F}_\ell^m$ are evaluated at the middle time level τ. By taking the transforms of the linear right-hand terms in the divergence and continuity equations, we get a coupled system analogous to that for the semi-implicit discretisation. We can solve it to get

$$\begin{aligned} s\,\widehat{\eta_\ell^m} &= \{\eta_\ell^m\}^{\tau-1} + \frac{1}{s}\,\{\mathcal{N}_\ell^m\}^\tau \\ s\,\widehat{\delta_\ell^m} &= \frac{1}{d'}\left(\mathcal{R}' + \frac{1}{s}\,\frac{\ell(\ell+1)}{a^2}\,\mathcal{Q}'\right) \\ s\,\widehat{\Phi_\ell^m} &= \frac{1}{d'}\left(\mathcal{Q}' - \frac{1}{s}\,\bar{\Phi}^*\,\mathcal{R}'\right) \end{aligned} \tag{15}$$

where

$$\begin{aligned} d' &= 1 + \bar{\Phi}^*\,\frac{\ell(\ell+1)}{a^2}\,\frac{1}{s^2} \\ \mathcal{R}' &= \{\delta_\ell^m\}^{\tau-1} + \frac{1}{s}\,\{\mathcal{D}_\ell^m\}^\tau \\ \mathcal{Q}' &= \{\Phi_\ell^m\}^{\tau-1} + \frac{1}{s}\,\{\mathcal{F}_\ell^m\}^\tau \end{aligned}$$

Comparing (14) and (15), we find close similarities between the two discretisations. Once we have computed the terms in (15), we use the inversion operator $\mathfrak{L}_N^*$ to compute the spectral coefficients at the new time $(\tau+1)\,\Delta t$, which is at a time $2\,\Delta t$ after the beginning of the time interval; for example

$$\{\eta_\ell^m\}^{\tau+1} = \mathfrak{L}_N^*\left\{\widehat{\eta_\ell^m}\right\}\Big|_{t=2\Delta t} = \frac{1}{N}\sum_{n=1}^{N} s_n\,\widehat{\eta_\ell^m}(s_n)\,e_N^{2\,\Delta t\,s_n}$$

3.4. Numerical simulations

To compare the LT method with the reference semi-implicit scheme, we use the test case suite of Williamson et al. (1992). In particular we consider Case 1 (advection of a cosine bell), Case 2 (steady zonal flow), Case 5 (flow over a mountain) and Case 6 (Rossby-Haurwitz wave).

A number of normalised error measurements are used for ease of comparison. Williamson et al. (1992) recommend the $l_1(h)$, $l_2(h)$ and $l_\infty(h)$ quantities, where $l_1(h)$ is the mean absolute difference from the reference, $l_2(h)$ is the root mean square difference, and $l_\infty(h)$ is the maximum absolute difference, each normalized by the appropriate measure of the reference solution. Normalised

invariants for mass and for total energy are also used to study the conservation properties of the schemes.

The LT version of STSWM was compared to the original semi-implicit version (the reference model) using the test cases outlined above. Unless otherwise stated, tests were carried out at a spectral T42 resolution with a 1200 second timestep. The default cutoff period for the LT method is $\tau_c = 6$ hours. For the inversion we test both $N = 8$ and $N = 16$. For Cases 5 and 6, fourth order diffusion is used in the semi-implicit runs, with the diffusion coefficients recommended by Jakob et al. (1993): for T42 simulations this is $5.0 \times 10^{15} \mathrm{m}^4\,\mathrm{s}^{-1}$.

For Cases 1 and 2, all schemes performed with high accuracy, and all were of comparable precision (for details, see Clancy (2010)). For Case 5, flow over an isolated mountain, there is no analytical solution. We compute errors by taking the 'true' solution from a T213 $\Delta t = 360$s reference run with a diffusion coefficient of $8.0 \times 10^{12} \mathrm{m}^4\,\mathrm{s}^{-1}$. The errors for the T42 simulations for 15 days, plotted in Figure 2 (left panel: l_2 error; right panel: l_∞ error), are of comparable magnitude for the reference and for the two LT forecasts (using $N = 8$ and $N = 16$ points). The three forecasts showed an almost identical decrease in mass, though at a negligible magnitude of $O(10^{-15})$ after 15 days. The deviation from energy conservation was also negligible for the three forecasts (Clancy, 2010).

For the Rossby-Haurwitz wave of Case 6, Jakob et al. (1993) recommend using shorter timesteps than for the other cases, due to the strong winds involved. The high-resolution 'true' solution is given by a T213 run with $\Delta t = 180$ seconds. The T42 simulations are run with a timestep of 600 seconds for 14 days. Errors are plotted in Figure 3. In this case we also ran two more LT forecasts, again using $N = 8$ and $N = 16$ but with a shorter cutoff period of 3 hours. We see that these forecasts are much closer to the reference than those with the 6 hour cutoff. All runs are comparable in terms of (negligible) mass loss. The LT $\tau_c = 3$ runs are best for energy conservation.

The value of the cutoff period τ_c is selected on the basis of numerical experimentation. There is no objective way to fix a precise value for this, and the optimal choice may vary with circumstances. However, the freedom to choose τ_c gives the LT scheme additional flexibility, not available in the semi-implicit scheme.

4. Simulation of Kelvin waves

Semi-implicit methods are popular due to their attractive stability properties. This is achieved at the expense of a slowing of the faster waves present in the system. This is not a serious issue if we are interested only in slower modes. There may, however, be cases where we wish to accurately simulate some of the faster waves. In these situations the semi-implicit approach may not be ideal. We investigate the effect of semi-implicit averaging on phase speed in the simplest context, and compare it to results using the LT discretisation. We then confirm the analytical results by simulating a Kelvin wave using the LT and semi-implicit schemes.

4.1. Phase error analysis

We begin with the one-dimensional oscillation equation

$$\frac{\mathrm{d}u}{\mathrm{d}t} = i\,\nu\,u \tag{16}$$

We follow the approach of Durran (1999) when analysing the two methods. We seek a numerical amplification factor, A, such that $u^{\tau+1} = A\,u^\tau$. Writing $A = |A|\,e^{i\,\theta}$, a sufficient criterion for stability is given by $|A| \le 1$. The phase is given by $\theta = \tan^{-1}\left(\Im(A)/\Re(A)\right)$. Following Durran, we define a relative phase change

$$R = \frac{\theta}{\nu\,\Delta t} \tag{17}$$

A numerical scheme is decelerating if $R < 1$.

We will compute the relative phase change for the semi-implicit scheme

$$\frac{u^{\tau+1} - u^\tau}{\Delta t} = i\,\nu\,\frac{u^{\tau+1} + u^\tau}{2}\,.$$

Evaluating the relative phase change R_{SI} using (17) we get

$$\begin{aligned} R_{SI} &= \frac{1}{\nu\,\Delta t}\,\tan^{-1}\left(\frac{\nu\,\Delta t}{1 - \nu^2\Delta t^2/4}\right) \\ &\approx 1 - \frac{(\nu\,\Delta t)^2}{12} \end{aligned} \tag{18}$$

for small values of $\nu\,\Delta t$. Clearly, the semi-implicit scheme decelerates waves.

We next apply the LT method to (16), to get

$$s\,\widehat{u} - u^\tau = i\,\nu\,\widehat{u}$$

Inverting analytically with the full integral $\mathfrak{L}^{-1}$ over a Δt interval yields $u^{\tau+1} = u^\tau\,e^{i\,\nu\,\Delta t}$. Thus we have an exact representation of the frequency. With the numerical inversion operator $\mathfrak{L}_N^*$ we get

$$u^{\tau+1} = u^\tau\,H_N(\nu)\,e_N^{i\,\nu\,\Delta t}$$

The relative phase change is given by

$$R_{LT} = \frac{1}{\nu\,\Delta t}\,\tan^{-1}\left(\frac{\sin_N(\nu\,\Delta t)}{\cos_N(\nu\,\Delta t)}\right) \tag{19}$$

where $\cos_N(\nu\,\Delta t)$ and $\sin_N(\nu\,\Delta t)$ denote, respectively, the real and imaginary parts of $e_N^{i\,\nu\,\Delta t}$. Taking a Taylor series yields

$$R_{LT} \approx 1 + \frac{N}{(N+1)!}\,(\nu\,\Delta t)^N \tag{20}$$

The details are given in Clancy (2010). The LT method gives a highly precise representation of phase speed, with an error due only to the discretisation of the inversion operator. This is clearly far more accurate than that for the semi-implicit case in (18). If, for example, we use $N = 8$ we get

$$R_{LT} \approx 1 + \frac{(\nu\,\Delta t)^8}{45360}$$

The scheme is marginally accelerating, but by a negligible amount.

In the next subsection we will consider a Kelvin wave with zonal wavenumber 5, with a period of about 6.7 hours. With a timestep of 30 minutes, the error in the semi-implicit scheme is then $R_{SI} \approx 0.98$ while a one hour timestep yields $R_{SI} \approx 0.92$. For the LT scheme with a 1800 second timestep, the error is $R_{LT} \approx 1.00000005$, completely negligible.

4.2. *Numerical integration for the Kelvin wave*

We now investigate the performance of semi-implicit and LT schemes in simulating Kelvin waves. These are eastward propagating waves, characterised by almost vanishing meridional wind. They are symmetric about the equator and decay with increasing latitude. They are known to play an important role in a number of atmospheric phenomena. Holton (1975) discusses their role in the dynamics of the Quasi-Biennial Oscillation (QBO) in the stratosphere. A comprehensive review may be found in Baldwin et al. (2001). Kelvin waves have also been shown to be important for the Madden-Julian Oscillation (Zhang, 2005). It is clearly vital, therefore, that these waves are accurately simulated.

Kasahara (1976) provides a description of the Hough modes along with details and code of a numerical method to produce them. This was used to generate initial conditions for STSWM. Since Hough modes are eigenfunctions for the linearised equations, they propagate almost linearly, without change of form, for small amplitudes.

For varying zonal wavenumbers m we compute the frequency of the Kelvin wave using the method of Kasahara. We use this to plot the relative phase changes for the semi-implicit and the LT method, given in (18) and (19) respectively. Figure 4 shows the errors plotted against the timestep for two wavenumbers: $m = 1$ and $m = 5$. For the two cases, the LT method (heavy black solid and dashed lines) are indistinguishable and appear to be almost exact. The deceleration is evident in the semi-implicit method (thin solid and dashed lines). As seen from (18), the slowing effect increases with larger timesteps and for the higher frequency of the $m = 5$ wave.

We compared three numerical simulations of Kelvin wave with zonal wave number $m = 5$. A mean height of 10 km was used with a wave perturbation amplitude of 100 m. For this value, the period is approximately 6.7 hours. All runs were carried out at a T63 spectral resolution. Figure 5 shows the hourly height at a single point close to the equator, ($0.0°$E, $0.9°$N), over the first 10 hours of the forecasts at $\Delta t = 1800$s. Here the phase speed differences are easily seen. The solid line marked 'Exact' is a sinusoidal wave with a 6.7 hour period, representing the analytical solution. Both LT forecasts, $N = 8$ (dashed line) and $N = 16$ (bold dashed), have nearly identical speeds closely matching the analytical solution. The semi-implicit solution (solid with circles) is visibly slowed.

From the previous analysis, we see that the amplification factor for the LT scheme is not equal to one. However, it is very close to one and no significant damping is observed in Figure 5.

5. Conclusion

We have developed a time integration method based on a modified inversion of the Laplace transform (LT). It can be configured to simulate low frequency components of the solution whilst eliminating unwanted high frequency oscillations. The method was compared to the semi-implicit (SI) approach. The SI method stabilizes high frequency gravity waves by averaging them. This has the effect of reducing the phase speed of the waves. The LT scheme has been shown to have smaller phase errors than the SI scheme when simulating a Kelvin wave. Since these waves are dynamically important, this is a significant advantage.

In this study we have combined the LT scheme with an Eulerian treatment of advection. Thus, the time step is limited by the strength of the ambient flow. In Part 2 we will combine the LT scheme with semi-Lagrangian advection, and show that it has additional important advantages over the semi-implicit method.

Acknowledgements

The STSWM model was originally developed at NCAR by J.J. Hack and R. Jakob and is available at `http://www.csm.ornl.gov/chammp/stswm/`. The Fortran 90 version used in this work is available from the ICON group at `http://www.icon.enes.org/`. This research was funded by the Irish Research Council for Science, Engineering and Technology Post-Graduate Scholarship Scheme and a UCD Research Demonstratorship.

References

Baldwin MP, Gray LJ, Dunkerton TJ, Hamilton K, Haynes PH, Randel WJ, Holton JR, Alexander MJ, Hirota I, Horinouchi T, Jones DBA, Kinnersley JS, Marquardt C, Sato K, Takahashi M. 2001. The Quasi-Biennial Oscillation. *Rev. Geophy.* **39**: 179–229

Clancy C. 2010. *A Laplace Transform Filtering Integration Scheme for Numerical Weather Prediction.* PhD Thesis, University College Dublin (Sept. 2010) `http://mathsci.ucd.ie/~plynch/candl.html`.

Clancy C, Lynch P. 2011. Laplace transform integration of the shallow water equations. Part 2: Semi-Lagrangian formulation and orographic resonance. Submitted to *Q. J. R. Meteorol. Soc.*

Daley R. 1991. *Atmospheric Data Analysis*. Cambridge University Press

Doetsch G. 1971. *Guide to the Applications of the Laplace and Z Transforms*. Van Nostrand Reinhold

Durran DR. 1999. *Numerical Methods for Wave Equations in Geophysical Fluid Dynamics*. Springer

Hack JJ, Jakob R. 1992. *'Description of a Global Shallow Water Model Based on the Spectral Transform Method'*. Technical Note NCAR/TN-343+STR. National Center for Atmospheric Research

Holton JR. 1975. *The Dynamic Meteorology of the Stratosphere and Mesosphere*. Meteolorological Monographs, Volume 15, Number 37, American Meteorological Society

Jakob R, Hack JJ, Williamson DL. 1993. *'Solutions to the Shallow Water Test Set Using the Spectral Transform Method'*. Technical Note NCAR/TN-388+STR. National Center for Atmospheric Research

Kasahara A. 1976. Normal Modes of Ultralong Waves in the Atmosphere. *Mon. Weather Rev.* **104**: 669–690

Lynch P. 1985a. Initialization using Laplace Transforms. *Q. J. R. Meteorol. Soc.* **111**: 243–258

Lynch P. 1985b. Initialization of a Barotropic Limited-Area Model Using the Laplace Transform Technique. *Mon. Weather Rev.* **113**: 1338–1344

Lynch P. 1986. *'Numerical Forecasting using Laplace Transforms: Theory and Application to Data Assimilation'*. Technical Note No. 48. Irish Meteorological Service

Lynch P. 1991. Filtering Integration Schemes Based on the Laplace and Z Transforms. *Mon. Weather Rev.* **119**: 653–666

Lynch P. 2006. *The Emergence of Numerical Weather Prediction: Richardson's Dream*. Cambridge University Press

Oppenheim AV, Schafer RW. 1989. *Discrete-Time Signal Processing.* Prentice Hall

Robert A. 1969. 'The integration of a spectral model of the atmosphere by the implicit method'. In *Proceedings of the WMO/IUGG Symposium on NWP, Tokyo*. Japan Meteorological Agency: VII.19–VII.24

Van Isacker J, Struylaert W. 1985. *Numerical Forecasting using Laplace Transforms*. Publications Serie A **115**. Institut Royal Meteorologique de Belgique

Van Isacker J, Struylaert W. 1986. Laplace Transform Applied to a Baroclinic Model. In *Short- and Medium-Range Numerical Weather*

Prediction, Proceedings of IUGG NWP Symposium. Meteorological Society of Japan, T. Matsuno, Ed., 831 pp : 247–253,

Washington WM, Parkinson CL. 2005. *An Introduction to Three-Dimensional Climate Modeling* (2nd edn.). University Science Books

Williamson DL, Drake JB, Hack JJ, Jakob R, Swarztrauber PN. 1992. A Standard Test Set for Numerical Approximation to the Shallow Water Equations in Spherical Geometry. *J. Comp. Phys.* **102**: 211–224

Zhang C. 2005. Madden-Julian Oscillation, *Rev. Geophys.* **43**: RG2003, doi: 10.1029/2004RG000158

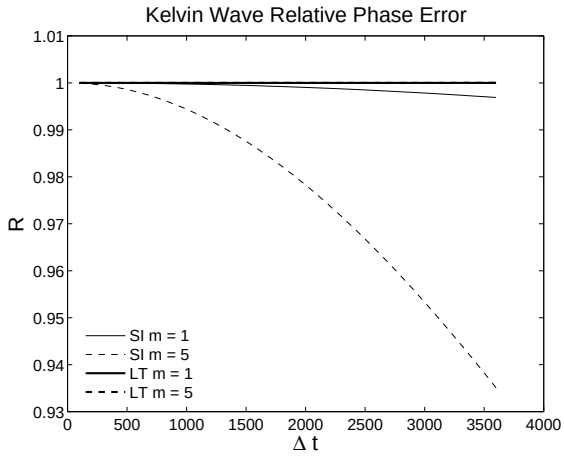

Figure 4. Relative phase errors for the semi-implicit (SI) and LT methods, for Kelvin waves of zonal wavenumbers $m = 1$ and $m = 5$. The errors in both LT runs are negligible.

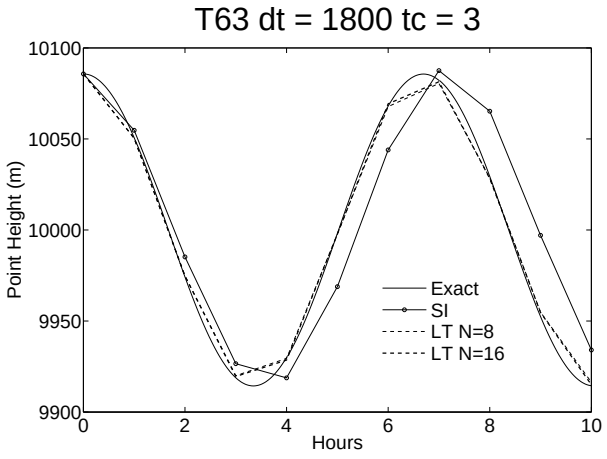

Figure 5. Hourly height at 0.0°E, 0.9°N over 10 hours with $\tau_c = 3$ hours

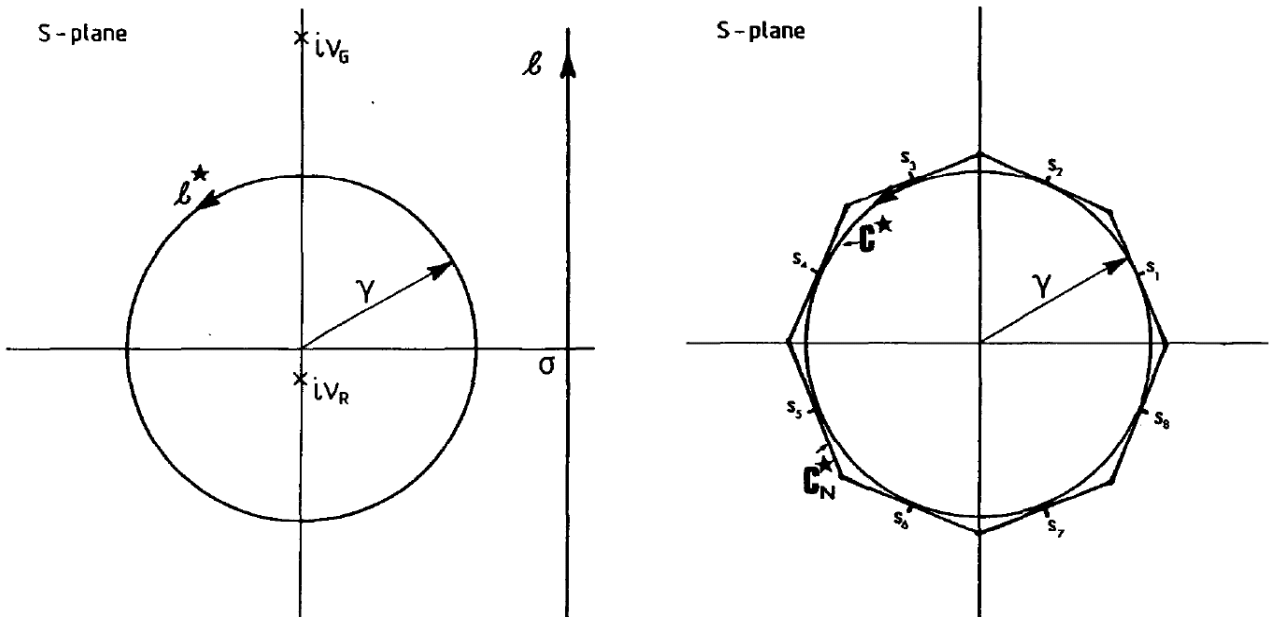

Figure 1. Left: The contour $\mathcal{C}^*$ replaces $\mathcal{C}$ for the modified LT inversion. Right: The numerical inversion is performed using $\mathcal{C}_N^*$. (From Lynch (1991), ©Amer. Met. Soc.)

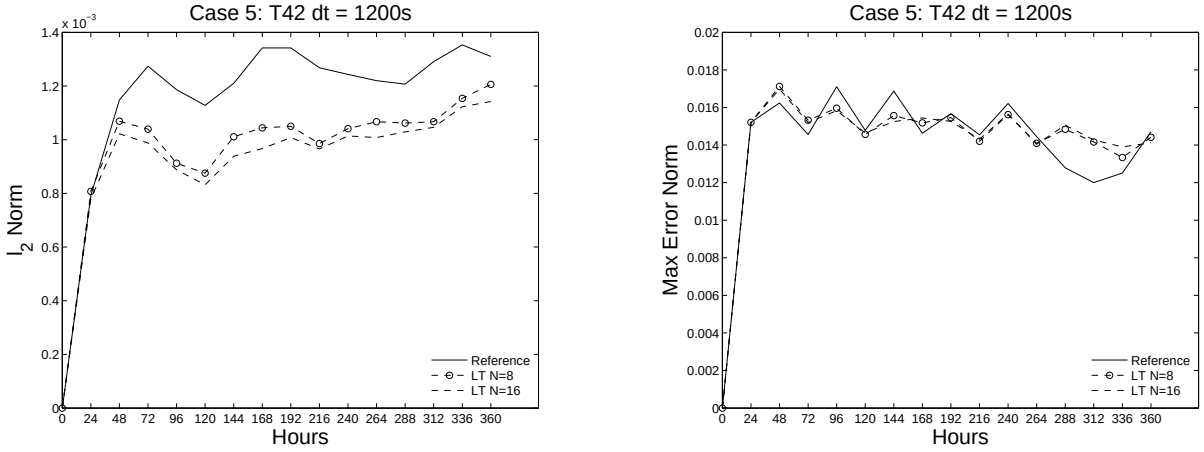

Figure 2. Case 5 at T42 and $\Delta t = 1200$s. l_2 error (left panel) and l_∞ error (right panel).

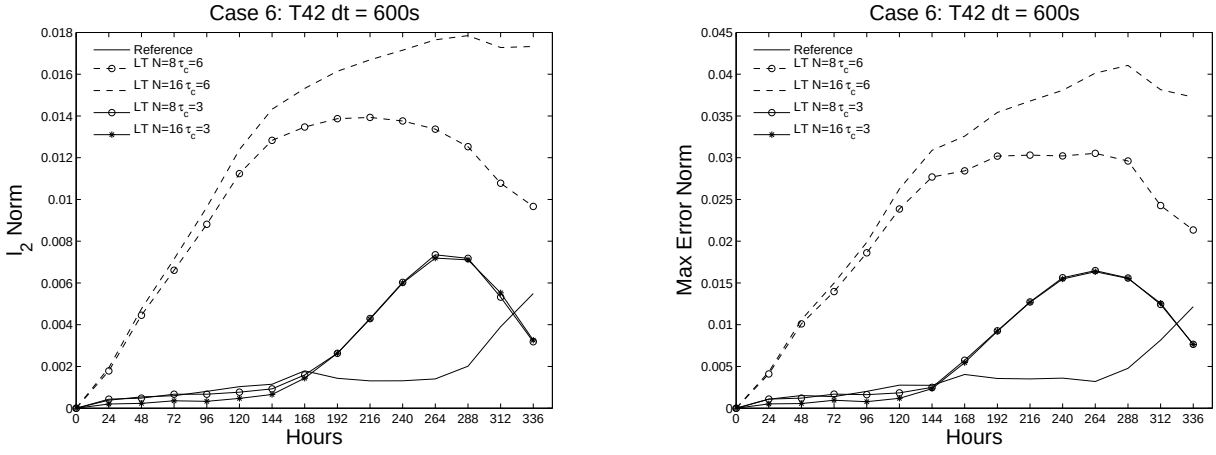

Figure 3. Case 6 at T42 and $\Delta t = 600$s. l_2 error (left panel) and l_∞ error (right panel).